Desalination 574 (2024) 117213

Contents lists available at ScienceDirect

Desalination

journal homepage: www.elsevier.com/locate/desal

Concentrate circularity: A comparative techno-economic analysis of membrane distillation and conventional inland concentrate management technologies

Varinia Felix, Mukta Hardikar, Kerri L. Hickenbottom *

Department of Chemical and Environmental Engineering, University of Arizona, Tucson, AZ 85721, United States
Water and Energy Sustainable Technology (WEST) Center, University of Arizona, Tucson, AZ 85745, United States

HIGHLIGHTS

- A techno-economic model of AGMD for inland concentrate management was developed and compared to conventional concentrate management technologies.
- At 0.90 \$/m^3, AGMD with low-grade heat is a viable and competitive technology to conventional concentrate management.
- The techno-economic framework and model developed can be used to assess MD treatment potential of various waste streams for different applications.

GRAPHICAL ABSTRACT

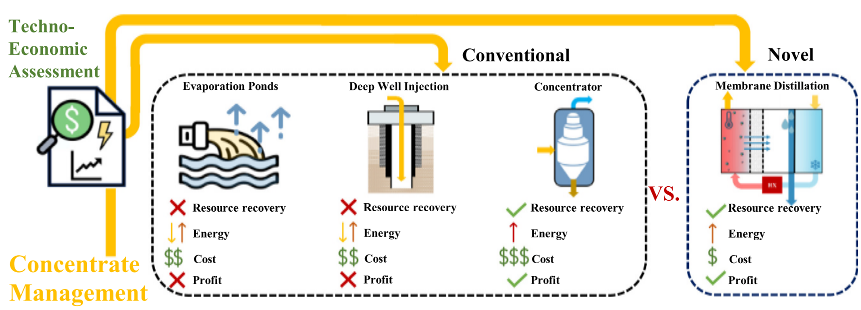

ARTICLE INFO

Keywords:
Concentrate management
Membrane distillation
Inland desalination
Resource recovery
Techno-economic assessment

ABSTRACT

Inland desalination with reverse osmosis (RO) offers a promising alternative to increase potable water resources. However, large volumes of concentrated brine are generated as a byproduct of the process. Concentrate disposal for inland regions displaces valuable water resources and can make up to 33 % of the total cost of desalination. Conventional disposal systems are limited by location, hydrogeology, climate, and policies, and few place value on resource recovery, thus limiting the implementation of desalination facilities in water-stressed regions. Membrane distillation (MD) is an alternative technology that can minimize disposal volume while maximizing water recovery for beneficial reuse. MD uses thermal energy gradients to desalinate the concentrate stream achieving near zero-liquid discharge. Furthermore, several MD configurations include heat recovery, making MD an energy-efficient alternative. A techno-economic assessment (TEA) of air-gap MD (AGMD) for RO concentrate management was performed and compared to three conventional concentrate management systems: evaporation ponds, deep-well injection (DWI), and concentration-crystallization. TEA results indicate that compared to DWI at 1.09 \$/m^3, evaporation ponds at 1.47 \$/m^3, and concentrators at 6.2 \$/m^3, respectively, AGMD is a competitive concentrate management technology producing water at 0.90 \$/m^3 when operating conditions are optimized and low-grade heat is available. When operating at high salinity (>70 g/L) the selection of operating conditions, specifically module length and circulating flowrate, is critical. Results of this study support the economic viability of AGMD in contrast to current industry standards and highlight the importance of resource recovery to promote a circular water-energy economy for regions relying on reuse and desalination.

* Corresponding author at: Department of Chemical and Environmental Engineering, University of Arizona, Tucson, AZ 85721, United States.
E-mail address: klh15@arizona.edu (K.L. Hickenbottom).

https://doi.org/10.1016/j.desal.2023.117213
Received 1 October 2023; Received in revised form 1 December 2023; Accepted 3 December 2023
Available online 7 December 2023
0011-9164/

Nomenclature

AGMD	Air Gap Membrane Distillation
AOP	Advanced Oxidation Process
CAPEX	Capital Expenditure
DCMD	Direct Contact Membrane Distillation
DI	Deionized Water
DWI	Deep Well Injection
GOR	Gained Output Ratio
GPM	Gallons Per Minute
HX	Heat Exchanger
LCCD	Levelized Cost of Concentrate Disposal
LCOW	Levelized Cost of Water
LGH	Low Grade Heat
MD	Membrane Distillation
MGD	Million Gallons per Day
O&M	Operation and Maintenance
PFTE	Polytetrafluoroethylene
PGMD	Permeate gap membrane distillation
RO	Reverse Osmosis
ROI	Return on Investment
STEC	Specific Thermal Energy Consumption
TDS	Total Dissolved Solids
TEA	Techno-Economic Assessment
US	United States
USD	United States Dollar
VMD	Vacuum Membrane Distillation
ZLD	Zero Liquid Discharge

1. Introduction

Concentrate disposal for inland regions can represent up to 33 % of the total cost of desalination, which constrains the implementation of inland desalination [1–4]. Typical recoveries for RO range from 50 to 80 % to maintain desired recovery and rejection, thus producing large volumes of concentrate rich in dissolved solids, organic matter, and pathogens to be managed [5,6]. In the U.S., the most widely used concentrate management systems include seawater or surface water discharge (45 %), sewer discharge (25 %), deep well injection (DWI, 17 %), land applications (7 %), evaporation ponds (4 %), and zero liquid discharge (ZLD, 1 %) [7].

Conventional inland concentrate management technologies are limited by location, hydrogeology, climate, and policies, and few place value on resource recovery, thus limiting the implementation of desalination facilities in water-stressed regions [2,8,9]. Although evaporation ponds are easy to construct and require low operation and maintenance, they are often limited to arid and semi-arid regions with high evaporation rates and low concentrate volumes [9–13]. DWI is primarily used for larger disposal volumes; however, their application is limited by potential contamination of groundwater and mineral resources, vulnerability to earthquakes, clogging and corrosion, public perception, and stringent regulations [9,12,14]. Additionally, evaporation ponds and injection wells take a disposal approach that does not place value on recovered resources. Thus, current research efforts focus on systems that move towards low energy and cost-effective near ZLD [15,16].

Conventional ZLD systems are often a combination of mechanical evaporators or concentrators, crystallizers, and solar evaporation [12,17–19]. In addition to their modularity and relatively small footprint, concentrator-crystallizer advantages include the ability to operate with high salinity streams, produce high purity water (<0.01 g/L TDS), and minimized waste [20]. However, concentrator-crystallizer systems have high energy requirements and capital investment [17].

In recent years, modular membrane-based technologies such as electrodialysis (ED), forward osmosis (FO), and membrane distillation (MD) have emerged as alternatives to conventional ZLD. However, ED has high energy requirements, removes only charged constituents, and is limited to concentrate salinities nearing 100–150 g/L [18,21,22]. FO and MD have salinity limits over 200 g/L [18,23,24]. However, the driving force in FO is limited when operating with high salinity streams, and the need to replenish the draw solution because of reverse solute permeation is an economic barrier [18,23,25,26]. MD has emerged as a promising energy-efficient technology for concentrate management because, compared to other membrane processes, it is not limited by high operating pressures (RO and nanofiltration), applied voltage (ED), and osmotic pressure gradients (FO) [27]. Furthermore, past studies have demonstrated that MD can concentrate hypersaline streams such as RO concentrate to near supersaturation while producing high-quality distillate, thus minimizing the volume of concentrate to dispose of [24,28–34].

Common MD configurations include direct contact MD (DCMD), permeate gap MD (PGMD), vacuum MD (VMD), and air gap MD (AGMD) [35]. Selection of MD configuration depends on the desired application, energy availability, and feed properties. PGMD requires a permeate recirculation system to maintain a constant temperature difference across the membrane. Additionally, permeate recirculation can be more energy intensive and increase fouling risks because of accumulation of impurities in the gap [35,36]. In VMD, the permeate side pressure is lowered via a vacuum, thus increasing the partial vapor pressure difference or driving force across the membrane; however, an external condenser is needed [36]. DCMD and AGMD have been studied for scale-up applications and are often preferred to VMD and PGMD because of their simplicity [29,35,37–43]. However, DCMD has higher conductive heat losses than AGMD because of the air gap acting as insulation [44], requiring the addition of external heat exchangers for scale-up applications [35,45,46]. Thus, AGMD has emerged as a promising configuration for full-scale applications because of its minimized conductive heat loss, low energy consumption, and internal heat recovery and potential to use low-grade heat (LGH) to drive the process [24,35,37,41,45,47–50].

In AGMD, a microporous membrane is in contact with a highly concentrated feed stream at an elevated temperature and a cooler condensing plate separated by an air gap (Fig. 1). The inlet condensing stream enters the condensing side of the membrane and is preheated along the length of the membrane before exiting the module to a heat exchanger. The preheated condensing stream is further heated via the heat exchanger and passed through the opposite side of the membrane producing a partial vapor pressure gradient that drives water vapor flux. Because theoretically only water vapor diffuses through the membrane pores, a high-quality distillate is produced.

Research efforts for scale-up of MD often focus on improving water production, energy efficiency, and mitigation of fouling and scaling via pre-treatment (i.e., ozonation, foam fractionation, air microbubbles, granular activated carbon, and chemical softening) [51–56]. Additionally, the technical efficacy of MD for concentrate management at the bench and pilot-scale has been demonstrated [28,29,33,45,57–60]. However, MD has received minimal attention in techno-economic studies when comparing its scale-up feasibility and cost competitiveness to conventional technologies for managing concentrate streams [49,60–63]. Previous studies have explored the economic feasibility of AGMD and water gap MD's (WGMD) to conventional desalination processes for various energy sources at a fixed salinity and operating conditions [64]. However, inland reuse and desalination have a wide range of salinity for feed and concentrate streams, which can have a significant effect on the cost of water production/concentrate disposal and

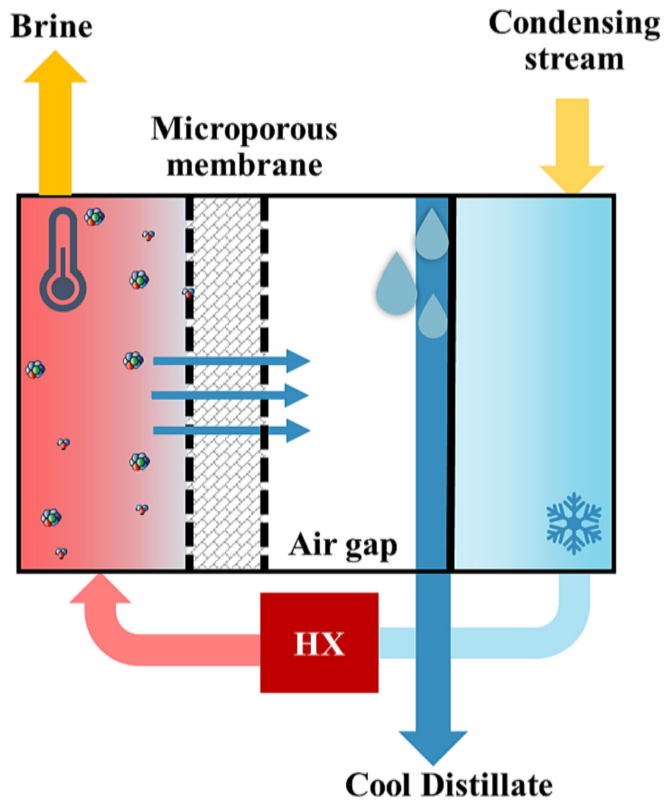

Fig. 1. System schematic for an AGMD System. In this configuration, the microporous membrane can be hydrophobic or omniphobic. In this energetically efficient AGMD configuration, the condensing stream is preheated along the length of the condensing side of the MD module before heated to the set temperature with an external temperature source and circulated on the feed side of the membrane module.

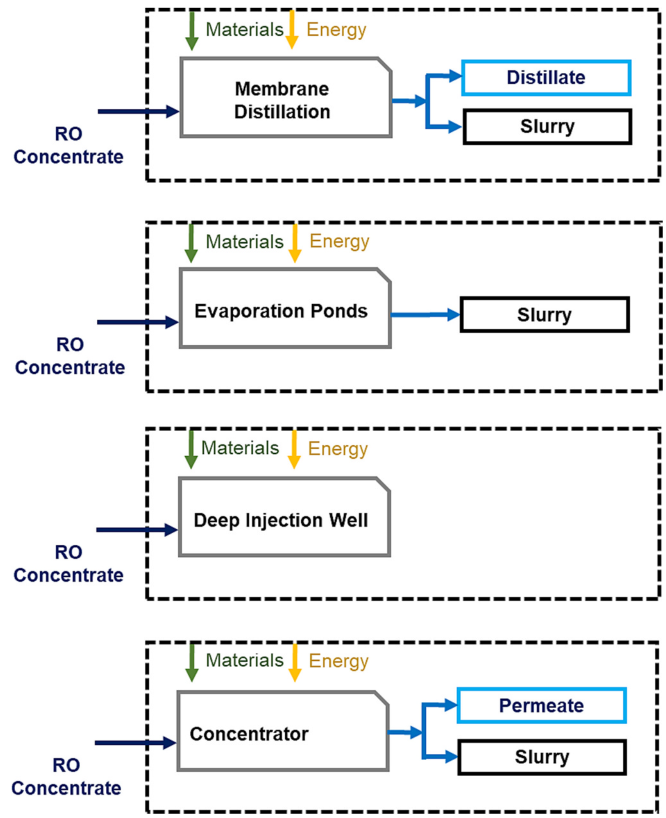

Fig. 2. System boundaries for AGMD, evaporation ponds, deep well injection, and concentrator systems are indicated by dashed lines. Inputs include concentrate stream; materials needed for new infrastructure, system equipment, and consumables; and energy inputs (i.e., electrical and thermal energy (LGH or external source)). Recovery of potable water and salts are considered as value-added products. System outputs include disposal of the remaining concentrate or slurry. Decommissioning of the systems after their lifespan is not included in the analysis.

therefore should be explored. Additionally, pilot-scale studies determined that module length, circulating flowrates and salinity range have a large impact AGMD energy efficiency and water production [45,65–68]. Hardikar et al. concluded that there is a specific operating flow rate to minimize the specific energy consumption for different salinities [58]. Because of the low transmembrane temperature differences and thus lower driving forces at the pilot-scale, operating conditions (i.e., flow rate, applied vacuum, and temperature difference) must be adjusted to achieve positive water flux [45,58,68–70]. Furthermore, although operating with shorter module lengths results in higher driving forces, longer module lengths is more energetically favorable [45,65]. Therefore, further investigation on the relationship between AGMD operating conditions (i.e., module length, salinity, flow rates) is critical for the advancement of MD as a technical and economic alternative to concentrate management.

The objective of this research is to fill this research gap by performing a comparative techno-economic assessment (TEA) of AGMD against conventional concentrate management systems, including evaporation ponds, DWI, and brine concentrator-crystallizers. An AGMD cost model is developed using cost correlations and an existing mechanistic model validated with pilot-scale experimental data [45,71]. The impact of select operating conditions including feed salinities, circulating flow rates, module lengths, and energy sources on AGMD system performance, energetics, and costs are evaluated. Sensitivity analyses are performed on each concentrate management system to evaluate how select operating conditions and major cost-contributing components impact system energetics and the levelized cost of water production (LCOW) or concentrate disposal (LCCD). Additional performance metrics, including freshwater production and resource recovery (i.e., salts) are included in the analysis. Finally, the best-case scenarios for each system are identified and compared to assess if MD is a competitive inland concentrate management system. The modeling framework can be applied for decision-making of concentrate management systems from brackish water desalination, produced water, and chemical and mining industries. Furthermore, this research supports exploring novel systems that reduce waste, increase recovery, and support water reuse efforts.

2. Methodology

All systems were modeled with a treatment capacity of 3785 m^3/day (1 MGD) of RO concentrate; this capacity was selected because of established system cost and manufacturing limitations for concentrate management technologies [12,17]. Systems were modeled with a range of salinities representing concentrate streams that have been investigated for treatment using MD (i.e. RO concentrate from reclaimed water, brackish water, or seawater; mining, oil and gas production, and other industrial processes) [23,72–76]. The plant life for each system is assumed to be 20 years, operating at 95 % capacity.

The boundaries of the concentrate management systems are shown in Fig. 2. System inputs include energy and materials needed during system construction and operation and maintenance (O&M). Recovered products (potable water and salts) are included as outputs for the AGMD and concentrator systems. End-of-life costs are outside of the scope of the study.

2.1. Modeling approach and system costing

Previously established models were used to assess the technical performance of each system. The cost model for each system includes capital (direct and indirect) and O&M costs. Direct capital costs include materials and equipment (e.g., membrane modules, pond liner, concentrators, piping, pumps, etc.), land purchasing, and clearing. Indirect capital costs refer to contingency, overhead, and engineering. O&M costs include labor, chemicals and materials, replacement parts, and energy. Costs were obtained from primary (i.e., literature and economic trends) or secondary sources (i.e., communications with vendors, engineering expertise, and manufacturer data). Indirect, control system, and piping costs are assumed to be a percent of the total direct cost for all systems [77].

2.1.1. Membrane distillation

The AGMD system was designed based on experimental data from bench and pilot-scale testing performed at the Water Energy and Sustainable Center at the University of Arizona and a previously established and validated AGMD model [45,57,71]. The experiments and modeling are based on a commercially available AGMD polytetrafluoroethylene (PFTE) membrane module (Aquastill, Sittard, NL). Model inputs include circulating flowrate, feed composition, operating temperatures, and module characteristics (i.e., number of channels, module area, and spacers). Therefore, the operating characteristics, including feed salinity, can be varied to evaluate the feasibility of AGMD for treatment of a wide range of feed streams. The circulating flowrates were selected considering the maximum hydraulic pressure losses not to be exceeded inside the module indicated by the manufacturer (600 mbar) and are supported by experimental data and literature [68,71,78,79]. The AGMD model assumptions include no heat loss to the environment, heat of vaporization to be the only contribution to heat duty, and that the concentrate stream is used for cooling, which is possible in AGMD configurations (Fig. 1). The evaporator and condenser inlet temperatures were fixed at 80 °C and 30 °C, respectively, to maximize the driving force, water vapor flux, and thermal efficiency according to manufacturer specifications and best operating parameters for scale-up projections of MD [45,78]. Model outputs include water vapor flux, STEC, and GOR.

The water vapor flux ($J_{w,\ AGMD}$, kg/m^2/s) is given by

$$J_{W,MD} = C^*(\Delta P) \tag{1}$$

where C (kg/m^2/s/Pa) refers to the membrane permeation coefficient and ΔP (Pa) to the partial vapor pressure difference across the membrane.

As MD utilizes mostly thermal energy to achieve the recovery of distillate, specific thermal energy consumption (STEC, kWh/m^3) and the gained output ratio (GOR) are used as performance indicators. STEC is defined as defined as the ratio of distillate produced to energy consumed:

$$STEC = \frac{Q_{thermal}}{\dot{V}_{dist}} = \frac{F_{feed}{}^*\rho\text{feed}^*C_P{}^*\Delta T_{HX}}{3.6^*10^6{}^*\dot{V}_{dist}} \tag{2}$$

where $Q_{thermal}$ is the heat consumed by MD, F_{feed} and F_{dist} (L/h) refer to feed and distillate flow rates, ρ_{feed} (kg/m^3) is the feed density, C_P (J/kg·K) is the heat capacity of water, ΔT_{HX} (°C) is the difference in temperature between the inlet and outlet of the MD heat exchanger, and $\dot{V}_{dist}$ is the distillate production volumetric flow rate. A low STEC is desirable as less energy is needed per unit volume of water produced. GOR is defined as the ratio of distillate produced and the energy required to convert 1 kg of water to steam:

$$GOR = \frac{F_{dist}{}^*\Delta H_v}{F_{feed}{}^*C\rho^*\Delta T} \tag{3}$$

where ΔH_v (J/kg) is the enthalpy of vaporization. A higher GOR is desired as values under one indicate no latent heat recovery. Although ΔHv and density vary slightly depending on the salinity and temperature, the relationship between GOR and STEC can be simplified to approximately 620 kWh/m^3 divided by the STEC:

$$GOR = \frac{\Delta H_V{}^*\rho_{feed}}{3.6^*10^6{}^*STEC} = \frac{620}{STEC} \tag{4}$$

An initial survey of STEC was performed for modules with an active membrane area of 7.2 and 26 m^2 (Supporting information Table S1). Results agree with previous research where longer membrane envelope lengths result in higher energy efficiency; therefore, the 26 m^2 module was chosen in this analysis [45].

The water vapor flux, STEC, and GOR are inputs to the economic model. Additional inputs for the techno economic model include but are not limited to plant capacity, pumping energy, plant availability, thermal energy source, hydraulic system, and pretreatment selection. Once the water vapor flux, STEC, and GOR are calculated, the required membrane area, number of modules, and system thermal energy needs and heat exchanger area are determined. Changes in thermal energy source (LGH or steam), circulating flow rates, salinity, membrane costs, and pretreatment options are presented as system sensitives on process costs.

Membrane module costs were obtained via personal communications with the pilot system manufacturers [80]. The baseline cost model considers the current market price for the 26 m^2 membrane module ($3000 USD). Based on manufacturer discussions, mass production of membrane modules is projected to reduce module cost by 10-fold; thus, a cost sensitivity was performed. Membrane replacement was estimated to occur every 10 years according to manufacturer specifications and priced as 10 %/year of the total capital costs for membrane modules [78]. Heat exchanger costs for AGMD were calculated according to the required system heating duty. Labor costs were determined by the volume of concentrate treated and estimated to be 0.03 $/m^3 [81]. The AGMD system was assumed to be located at the end of the RO treatment facility; therefore, pumping costs are limited to the circulation of the brine stream. The selected pretreatment is ozonation with doses between 0.1 and 0.4 mg O_3/mg DOC ratios have been reported to reduce organic fouling potential by altering NOM size distribution and functional groups, thus reducing foulant-membrane interactions [53,82]. Additional information on the pretreatment system, including dose selection and cost correlations, is included in the supporting information (Table S2).

2.1.2. Evaporation ponds

To model the evaporation pond system, pond filling (t_f) and saturation times (t_s) in days given by Eqs. (5) and (6) were estimated through an iterative process of varying evaporative areas and typical dike heights [17]. Because the pond is filling while the concentrate evaporates, the ratio between pond filling and saturation closest to unity was selected to maximize continuous evaporation and minimize pond area and number of ponds. The pond filling (t_f) time is a function of the pond volume (V_t, m^3), equilibrium concentration (C_e, mol/m^3), initial concentration (C_0, mol/m^3), and flow rate of the inlet stream (q_0, m^3/day):

$$t_f = \frac{V_t{}^*C_e}{C_0{}^*q_0} \tag{5}$$

The saturation time (t_s) is a function of the volume of concentrate at the end of the drying process (V_f, m^3), initial volume of the pond before drying (V_0, m^3), surface area of the evaporation pond (A, m^2), average rainfall rate (R, m/day), evaporation rate of freshwater (E_0, m/day), and saturation concentration in the pond (C_{sat}, mol/m^3):

$$t_s = \frac{V_f - V_0}{A \times R - A \times E_0(1 - C_{sat})} \tag{6}$$

The evaporation pond cost model inputs include capital (i.e., land,

Table 1
General and system-specific financial assumptions used to develop the cost models. All costs are presented in 2023 USD.

Attribute	Value	Unit	Reference
Inflation rate (n)	3 %		Assumed
Interest discount rate (i)	10 %		Assumed
Amortization factor (a)	12 %		i × (1 + i) n ÷ ((1 + i) n − 1)
Land cost	1.44	$/m²	[91]
Land clearing	0.25	$/m²	[17]
Electricity cost	0.07	$/kWh	[27]
Steam cost	0.14	$/m³	[28]
Pump efficiency	70 %		Assumed
Water market price	0.50–3	$/m³	[20,92]
Water reservoir	76–95	$/m³	[92]
Membrane distillation			
Spares	0.05	$/m³	[81]
Labor	0.04	$/m³	[81]
Evaporation pond			
Liner cost	3–15	$/m²	[17]
Concentrator			
Concentrator energy consumption	21–24	kWh/m³	[20,92]
Labor cost	40	$/h	[77]
Chemicals	0.0191	$/m³	[92]
Spares and replacement	0.031	$/m³	[92]

Table 2
Cost correlations used in the techno-economic model.

Attribute	Equation	Reference
General		
Pump design	$C_{CPump} = I \times f_1 \times f_2 \times L \times 81.27(Q \times P)^{0.39}$	[77]
Concentrate transport pump ($)	C_{Pump} = Hp Required * $Hp	[93]
Storage reservoir ($)	$C_{Reservoir} = 0.5 \times$ Reservoir Cost ($/m³) × Capacity (m³)	[92]
Piping and fittings ($)	$C_{Piping} = 12.5 \times$ CAPEX	[94]
Engineering ($)	$C_{Eng} = C_D \times 0.1$	[95,96]
Contingency ($)	$C_{Contingency} = C_D \times 0.1$	[95–97]
Control System ($)	$C_{Control} = 5\text{–}10\,\%\ C_D$	[77]
Indirect Auxiliary ($)	$C_I = C_{Eng} + C_{Contingency} + C_{Control}$	
Total capital ($)	$CAPEX = C_D + C_I$	
Normalized capital cost ($/m³)	N_{CAPEX} = CAPEX*a/PA × Plant Capacity (m³/day) × 365	
Normalized O&M ($/m³)	$N_{O\&M}$ = O&M/PA × Freshwater recovery × 365	
LCOW/LCCD ($/m³)	$N_{CAPEX} + N_{O\&M}$	
Membrane distillation		
Heat exchangers ($)	$C_{HX} = 300 \times A_{HX} \times 10.77^{\ 0.6907}$	[98]
Steam HX ($)	$C_{HXSteam} = A_{HX} \times HX_{Steam}$ ($/m²)	[81]
Civil Work ($)	$C_{Civil} = 12{,}253 \times \Sigma A_{Mem}^{0.57}$	[99]
Membrane modules ($)	C_{Module} = Cost of module ($) × Number of modules	
Membrane replacement ($ yr–1)	$C_{MRep} = 0.1 \times C_{Module}$	
AGMD labor and spares ($yr–1)	$C_{AGMD\text{-}Labor\text{-}Spares} = (S_L + S_S) \times PA \times Q \times 365$	[81]
Thermal energy ($)	$C_{Thermal}$ = Thermal demand (kWh/m³) × steam cost ($/ton) × PA factor × 365	

Table 3
Parameters used for the design of the concentrate management systems.

Membrane distillation		
Operating feed flow rate	600–14,600	L/h
Feed salinity	15–140	g/L as NaCl
Membrane area	26	m²
Feed inlet temperature	80	°C
Condenser inlet temperature	30	°C
Membrane module cost	300–3000	USD
Thermal energy source	LGH, steam	
Evaporation pond		
Feed salinity	15–140	g/L as NaCl
Evaporation rate	1–4.5	m/year
Deep well injection		
Well diameter	16	cm
Well depth	305–2438	m
Transport distance	1.6–33	km
Concentrator		
Concentrator flow rate	3785	m³/day
Feed salinity	6.3–250	g/L as NaCl
Recovery	85–98	%

earthwork, and liner) and O&M costs (i.e., slurry removal and water quality monitoring). Land costs include pond evaporative area, roads, fencing, and clearing and are calculated based on pond area, land value, and land type [17]. Liner requirements and costs are estimated based on liner thickness and evaporative area. The base-case cost model uses a 60 mm high-density polyethylene liner. Installation costs are calculated according to liner thickness and are estimated at 0.1 $/mil thickness per m² [17]. All capital costs use empirical correlations that include labor and materials needed for the evaporation pond construction (i.e., fencing and roadways, control systems) and pumps. O&M costs include general monitoring of the evaporation pond, transportation of the RO concentrate to the pond and slurry removal at the end of the drying process at a cost of 50 $/ton of slurry removed. The baseline for the evaporation pond cost estimations uses a conservative pumping distance of 0.40 km (0.25 mi), as geo-mapping of various treatment facilities using evaporation ponds in the southwestern U.S. indicate that water treatment facilities with evaporation ponds are generally within <0.5 km of the installations (i.e., Hayden Plant in Colorado, the Reverse Osmosis Recharge Facility & Brine in Arizona and the Fred Hervey Water Reclamation in Texas).

2.1.3. Deep well injection

The complex nature of deep well design depends on hydrogeologic and policy constraints. A previously established cost modeling approach for Class I wells was used as the basis for this analysis, with modifications including pumping and land costs [17]. A variety of representative depths from 0.7 to 3 km that fall within typical well depths in the U.S. were considered in this analysis [17]. The piping diameter was determined based on suggested downflow injection velocity recommendations ranging between 2.5 m/s and 3 m/s. Similarly, representative distances were selected by reviewing current injection wells used for concentrate disposal in the U.S. with similar characteristics [83].

Capital costs for DWI include mobilization and demobilization, monitoring, drilling, grouting, casing, piping, packing seal (based on well diameter), and pump equipment (based on transport distance) [17]. General O&M costs were calculated as a percent of the total capital costs for the system in accordance with published values from the Kay Bailey Hutchison desalination plant in El Paso, Texas, which has a similar

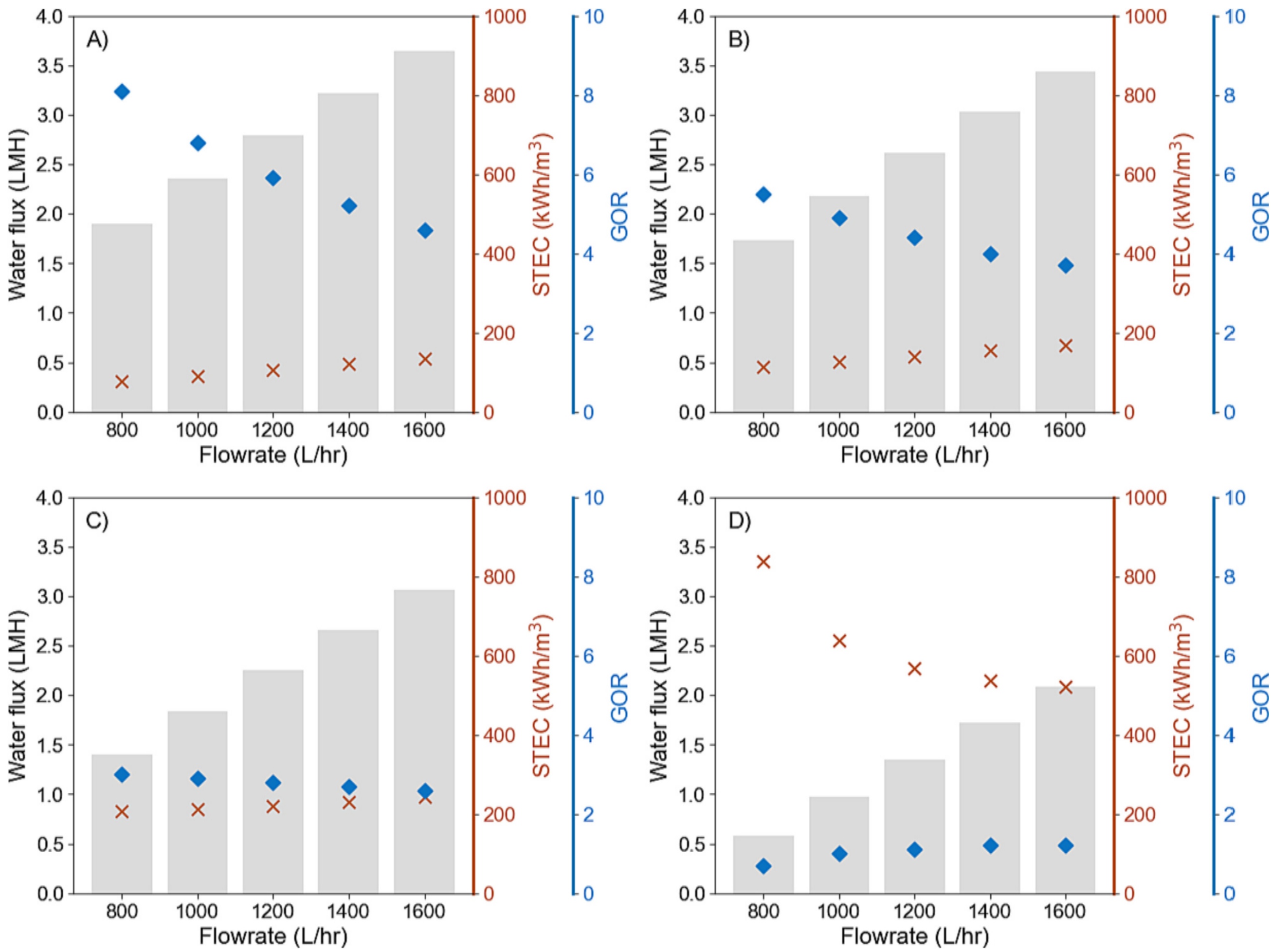

Fig. 3. AGMD Water vapor flux and STEC as a function of operating flow rate for feed salinities of A) 15 g/L, B) 35 g/L, C) 70 g/L, and D) 140 g/L as NaCl. Corresponding GOR and STEC are shown on the secondary axis. The system was modeled using a 26 m^2 active area PFTE module and evaporator and condenser inlet temperatures of 80 °C and 30 °C respectively.

concentrate disposal capacity of three deep injection wells with a maximum capacity of 11,356 m^3/day (3 MGD, ≈1 MGD per injection well) and have the same Köppen-Geiger climate classification zone B for dry climate [84]. General O&M expenses consider monitoring the injection zone and physical and chemical pretreatment of the injectate to account for potential mineral precipitation, injection tube clogging, scaling, and fouling [17,19]. Pumping O&M costs depend on the concentrate transport distance; representative distances were selected by reviewing current injection wells used for concentrate disposal in the U.S. with similar capacity and climate characteristics [85–87].

2.1.4. Concentrator

The concentrator design was based on a previously developed cost estimation and vendor-available information from HPD-Veolia Water Solutions [88]. The cost of commercially available equipment based on capacity from 0.3 to 2.6 m^3/min (86–694 gpm) and salinity (6.3–28 g/L) were used to develop empirical cost correlation inputs for the cost model. Capital costs for the concentrator include concentrator equipment, pumping equipment, piping, and installation costs. O&M costs include energy requirements, labor, spares and replacements, and chemicals needed for cleaning based on a 180-day period [20]. The concentrator was modeled with recoveries ranging from 85 % to 98 %. Because concentrator equipment can reduce up to 98 % of the initial feed volume [88], including a crystallizer would only benefit when a potential profit analysis indicates that annual salt recovery would offset crystallizer equipment and operational costs. Because of the low market value for salts in the modeled solution [12], using a crystallizer was not included in the concentrator system. Dry solid production from the concentrator system for the feed salinities analyzed (6.3–28 g/L) ranges between 26 and 118 metric tons per day. O&M costs for spares and chemicals are assumed to be 1–3 % of the concentrator equipment [20,89]. Labor requirements were calculated according to equipment type and are estimated to be approximately 10,236 man hours/year at 25 $/h [90]. The concentrator system is assumed to be located at the end of the RO treatment facility. Therefore, pumping requirements were considered as part of the existing infrastructure.

2.2. Life cycle costing

General and system-specific financial assumptions are summarized in Table 1. Capital and O&M cost correlations are presented in Table 2. All costs were brought to present-day values (2023 USD). The annual inflation rate is assumed to be constant at 3 % over the plant life period to calculate LCOW ($/$m^3$) for systems that place value on water recovery (AGMD and concentrator) and LCCD for conventional concentrate management (DWI and evaporation ponds) to reflect the financial implications of the resource disposal approach. System-specific cost correlations for conventional concentrate management technologies (i.e., evaporation ponds, DWI, and concentrator) are presented in detail in the supporting information (Table S3).

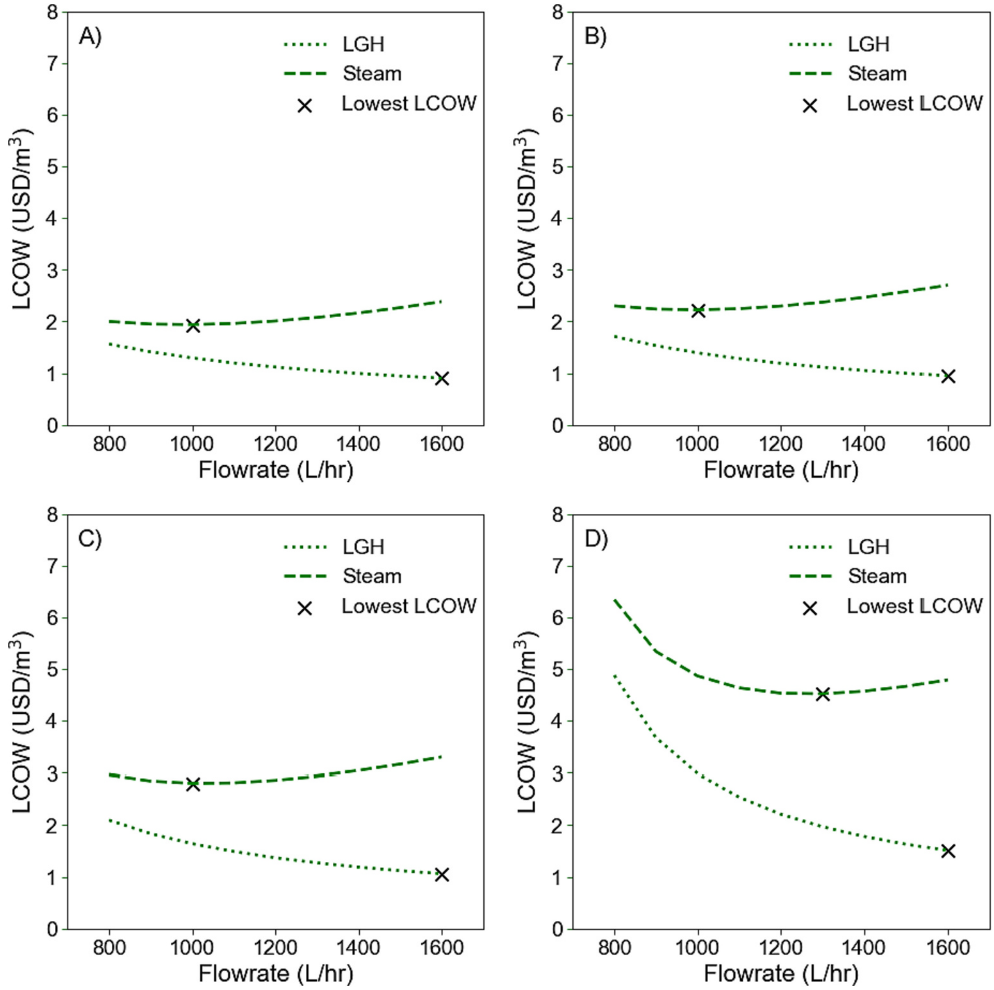

Fig. 4. Water vapor flux and LCOW as a function of operating flow rates for feed salinities of A) 15 g/L, B) 35 g/L, C) 70 g/L, and D) 140 g/L as NaCl. The solid line refers to water vapor flux, while the dashed line refers to the LCOW. For LGH, the lowest LCOW occurs at 1600 L/h. The lowest LCOW depends on feed salinity and circulating flow rate when an external thermal energy source is needed. For feed salinity up to 70 g/L, the lowest LCOW occurs at 1000 L/h, while at the highest salinity (140 g/L), the lowest LCOW is a tradeoff between membrane area and energy requirements, and it occurs at 1300 (L/h).

2.2.1. *Sensitivity analysis*

Sensitivity analyses were performed to analyze the effects of variable operating parameters on system performance (e.g., specific energy consumption, levelized cost of disposal, etc.). Sensitivity parameters were selected based on system variables that had the largest fractional contributions to cost. Circulation rate, membrane module cost future projections [80], and thermal energy source were selected as AGMD sensitivities. Evaporation rate and pumping transport distance were explored for the evaporation pond. Depth and concentrate pumping distance were selected for DWI sensitivities. For the concentrator system, salinity and recovery rater were considered. System-specific input parameters and sensitivity ranges for each system are summarized in Table 3.

3. Results and discussion

3.1. *Membrane distillation*

The AGMD water vapor flux, STEC, and GOR as a function of circulation flow rate for different feed salinities is shown in Fig. 3. The water flux decreases as the salinity increases because of the reduced water activity, thus reducing the partial vapor pressure difference across the membrane. In general, operating at higher circulating flow rates reduces concentration polarization, resulting in an increased driving force, decreased conductive heat loss (i.e., larger temperature gradient across the membrane), and thus an increase in water flux. Similarly, the STEC for each unique circulating flowrate increases with salinities up to 70 g/L. For example, at a fixed flowrate of 800 L/h and salinity of 140 g/L the STEC is 4-fold higher than at medium salinities (70 g/L) and 11-fold higher at low salinities (15 g/L). For low to medium salinity (15–70 g/L), increasing circulating flowrate results in an increased rate of thermal energy consumption, thus reducing the driving force, resulting in an increase in STEC; in other words, the lowest STEC occurs at the lowest circulating flowrate. In contrast, at the highest feed salinity of 140 g/L, the opposite trend is observed; a minimum STEC occurs at the highest circulating flow rate because an increase in salinity requires a larger temperature difference to overcome the decrease in vapor pressure, which occurs at higher flow rates [45]. In other words, because of the decreased partial vapor pressure of the feed stream at higher salinities, more heat input (achieved by increased circulating flow rate) is needed to increase the driving force and water production.

STEC and GOR are inversely correlated; as STEC increases, more heat is required to achieve a given amount of water vaporization, resulting in a decrease in GOR. For example, for feed salinities between 15 and 70 g/L, the lowest STEC and highest GOR occur at the lowest circulating flow rate of 800 L/h. However, at the highest salinity, operating at low circulating flow rates results in lower energy recovery and water fluxes; therefore, the minimum STEC and maximum GOR occur at the highest

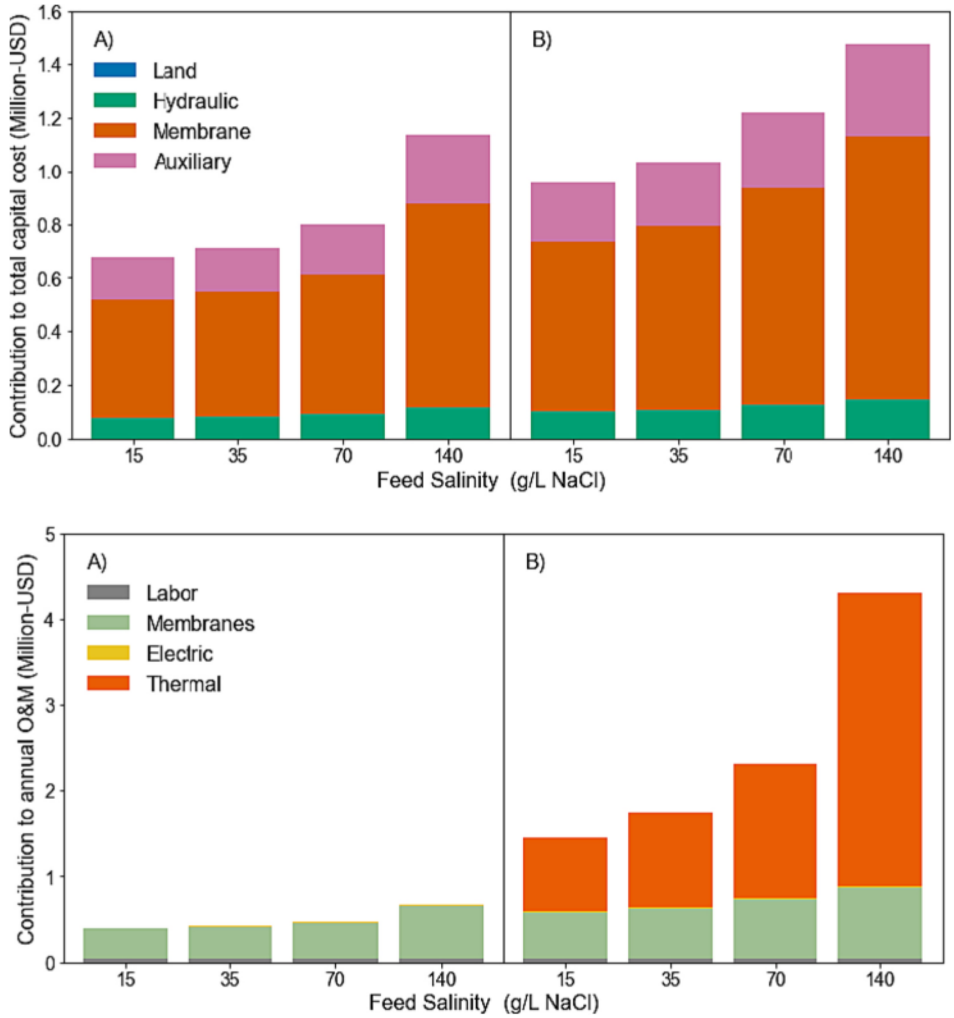

Fig. 5. Contribution to total capital investment and annual O&M cost by components of the AGMD system. Results are grouped according to thermal energy source: A) LGH and B) steam. Results shown represent the operating flow rate where the LCOW is minimized, for LGH this happens at a circulating flow rate of 1600 L/h and for an external energy source at 1000 L/h for feed salinity up to 70 g/L and 1300 L/h for 140 g/L. The membrane subsystem, which includes membrane modules, installation, heat exchangers, coolers, and circulating pumps comprise >60 % of the total capital investment for any system regardless of feed salinity or thermal energy source. When LGH is available, membrane replacement has the largest contribution to O&M costs. When LGH is unavailable, introducing a thermal energy supply subsystem contributes the most to O&M costs regardless of feed salinity.

circulating flow rate of 1600 L/h.

The water vapor flux and LCOW as a function of circulating flow rate for different feed salinities and energy sources is shown in Fig. 4. Regardless of the thermal energy source, an increase in salinity translates to a decrease in water vapor flux, an increase in required membrane area, and an increase in LCOW. In cases where LGH is available, operating at increased circulating flow rate is desirable as operational costs associated with thermal energy supply are negligible and distillate production is maximized, resulting in lower membrane area requirements to meet the desired water production and an overall lower LCOW. For example, when LGH is the energy source, operating at 1600 L/h results in a LCOW range from 0.90 $/m^3 to 1.51 $/m^3 with increased salinity (15–140 g/L NaCl).

When steam is the thermal energy source, the desired operating conditions are a tradeoff between energy efficiency (i.e., STEC and steam purchased) and water production (i.e., water vapor flux and membrane area). Operating at lower flow rates results in decreased water vapor flux and higher STEC, thus increasing the total membrane area and steam volume required. Conversely, operating at higher flow rates results in increased water vapor flux and lower STEC, thus decreasing total membrane area and volume of steam required.

For feed salinities of 15, 35, and 70 g/L, when steam is the thermal energy source, the minimum LCOW occurs at 1000 L/h while at higher salinity (140 g/L) the minimum LCOW occurs at 1300 L/h. When an external thermal energy source is required, the LCOW ranges from 1.9 to 4.5 $/m^3 for 15 and 140 g/L salinity, respectively. In general, operating at increased feed salinities translates to increased operating costs because of higher total membrane area requirements, higher STEC, lower energy efficiency, and increased steam volume required. Beyond the minimum LCOW flow rate, the economic advantages of lower membrane area requirements, which reduce capital and module replacement expenses (O&M), are offset by the increased costs associated with steam purchasing (O&M expenditure).

The fractional contribution to AGMD capital and O&M costs for operating flow rates that result in a minimum LCOW is shown in Fig. 5. Subsystems include land costs (i.e., purchasing and clearing), hydraulic system (i.e., reservoir, piping, and feed pumps), AGMD system (i.e., membrane modules, installation, heat exchangers, coolers and circulating pumps), and auxiliary costs (i.e., engineering, contingency, and control systems). Because of the low water vapor flux and the high cost of modules currently available in the market, the required membrane area constitutes the largest portion of the capital investment for the AGMD system and the total capital investment ranges from 65 to 67 % at 15 g/L and 140 g/L, respectively. O&M subsystems are grouped as

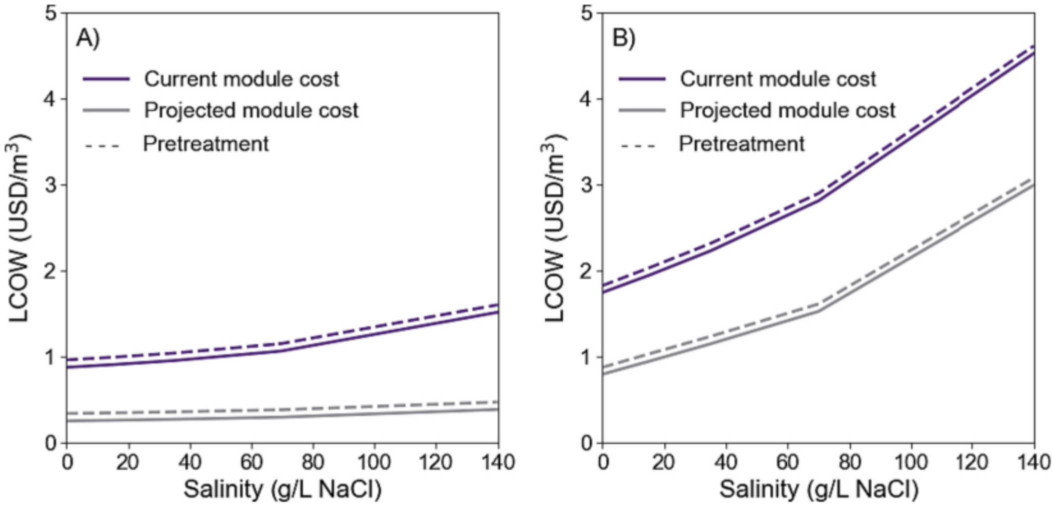

Fig. 6. LCOW for various salinities, considering the implementation of a pretreatment step and future membrane module costs projections at mass production. Results are grouped according to thermal energy source supply by A) LGH and B) Steam. The evaporator and condenser inlet temperature are fixed at 80 °C and 30 °C, respectively.

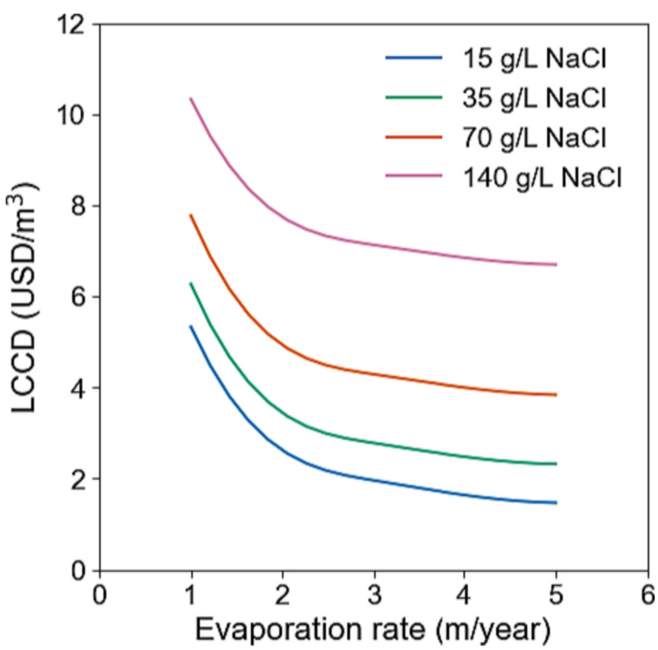

Fig. 7. Levelized Cost of Concentrate Disposal LCCD in $/m3 for an evaporation pond with dike height of 2.4 m (8 ft) and minimal pumping distance of 0.4 km (0.25 mi) as a function of evaporation rate and feed salinity. LCCD increases with salinity and decreases at higher evaporation rates.

electric, thermal, membrane, and labor costs. In cases where LGH is available, membrane replacement costs range from 87 to 92 % of the O&M, the majority of the O&M costs, as thermal energy costs are neglected. However, when LGH is not available, thermal energy requirements are the main contributor to O&M. The thermal subsystem energy requirements increase with feed salinity ranging from 60 to 80 % for a feed stream of 15 and 140 g/L, respectively, while membrane replacement contribution decreases to 19–51 % from low to high salinity (15–140 g/L NaCl).

The LCOW as a function of feed salinity using projected costs of membrane modules at mass production, with and without pretreatment for prevention of organic membrane fouling, is shown in Fig. 7. Mass production of membrane modules is projected to reduce the contribution of module cost by 10-fold, which results in a 72–75 % decrease in LCOW when using LGH for low (15 g/L) to high salinity (140 g/L), respectively, and a 34 to 52 % decrease in LCOW when using steam as the thermal energy supply for low (15 g/L) to high salinity (140 g/L), respectively. Conversely, the integration of pretreatment in the AGMD system results in a 6 to 10 % increase in current LCOW for cases utilizing LGH and a 2 to 4 % increase in LCOW when steam is the thermal energy source for low (15 g/L) and high (140 g/L) salinity, respectively. Because successful pretreatment could potentially reduce membrane fouling, there is potential for longer operational periods between membrane maintenance and/or replacement, which could translate into a reduction of the membrane subsystem O&M costs, thus potentially offsetting the increase in LCOW. A similar outcome would be expected for pretreatment and cleaning strategies that mitigate or prevent scaling of the membrane modules. The membrane subsystem is the major capital cost contributor regardless of thermal energy source. The membrane subsystem is also the highest cost contributor to O&M, representing the highest cost when LGH is available and the second highest when steam is used. Therefore, improvement of membrane parameters that advance performance, specifically enabling higher water vapor flux and including pretreatment systems that prolong membrane life and reduce membrane replacement rates could result in lower LCOW (Fig. 6).

3.2. Evaporation ponds

The LCCD as a function of evaporation rate (1–5 m/year), and feed salinity (15–140 g/L of NaCl) for ponds with dike height of 2.4 m (8 ft) and minimal pumping distance of 0.4 km (0.25 mi) is shown in Fig. 7. Dike height was selected as the midpoint within typical recommended dike depth ranges of 1.2–4 m (4 to 12 ft), to provide a conservative estimation. Evaporation rate and feed salinity highly influence the cost as they define evaporative area and volume of slurry to be removed at the end of each drying cycle.

For a low salinity stream (15 g/L NaCl) an increase in evaporation rate from 1 to 5 m/year decreases the LCCD from 5.33 $\$m^3$ to 1.47 $\$m^3$ – a by nearly 73 % decrease. While for the highest modeled salinity of 140 g/L increasing the evaporation rate from 1 to 5 m/year results in a decrease in LCCD from 10.33 $\$/m^3$ to 6.7 $\$/m^3$ (35% decrease); in both cases the decrease of LCCD is a result of lower evaporative area requirements at higher evaporation rates. Similarly at any fixed evaporation rate, an increase in salinity results in a higher LCCD because of the increase in volume of slurry to be removed at the end of the drying

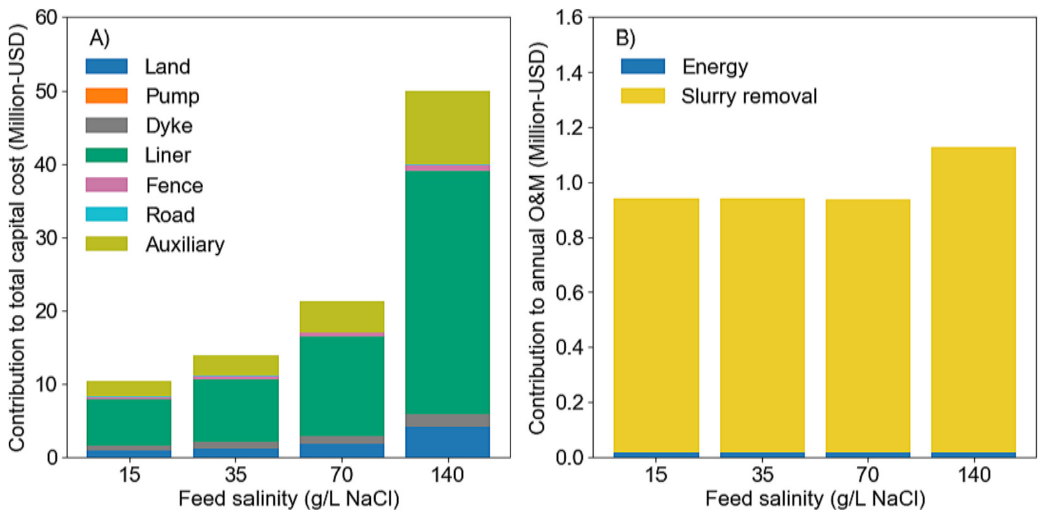

Fig. 8. Fractional contribution to A) Capital and B) Annual O&M costs for evaporation ponds at a fixed evaporation rate of 5 m/year as a function of feed salinity. In all cases, liner costs (Including materials and installation costs) represent the largest contribution to capital cost with a range from 60 to 67 % of the initial investment, followed by auxiliary costs which include contingency, engineering, and control system costs. Slurry removal makes up most of the O&M expenses (98 to 99 %) due to the passive nature of evaporation ponds as a concentrate disposal system.

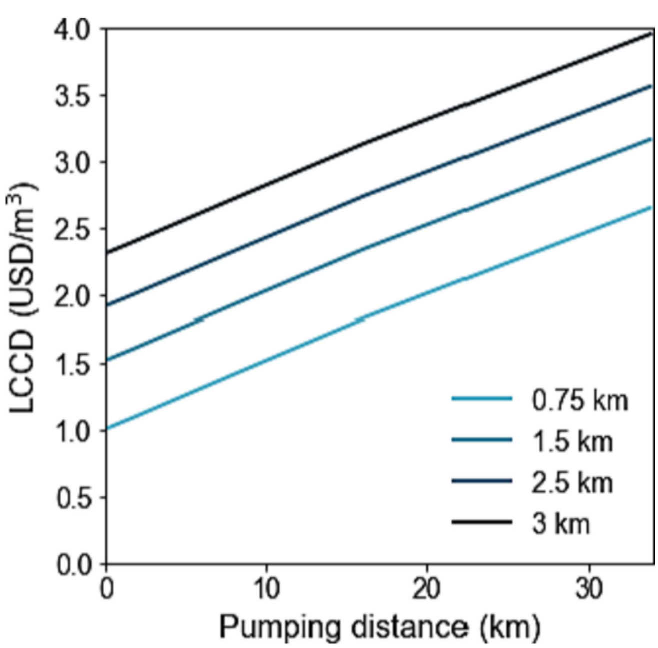

Fig. 9. LCCD for a DWI with capacity of 3785 m^3/day as a function of concentrate pumping distance and well depth. LCCD increases linearly with pumping distance and well depth because of larger excavation and operational energy requirements as depth and distance increase.

process. Therefore, evaporation ponds are most cost effective at high evaporation rates, lower salinities, and minimized concentrate volumes. The best-case cost scenario for evaporation ponds at a LCCD of 1.47 $/$m^3$ is for the scenario with the shortest concentrate transport distance (0.4 km), highest evaporation rate (5 m/year), and lowest feed salinity (15 g/L).

The fractional contribution to capital and O&M cost for an evaporation rate of 5 m/year, transport distance (0.40 km), and various feed salinities is shown in Fig. 8. Capital cost for evaporation ponds is comprised of land (purchasing and clearing), pump equipment, dike excavation, liner (purchasing and installation), fencing, road, and auxiliary costs. Liner costs have the highest contribution to capital costs and range from 60 % to 67 % depending on feed salinity. General O&M costs consist of slurry removal and concentrate transport energy requirements. The volume of slurry at the end of the drying process has the greatest effect on O&M and is proportional to the concentration of the feed, making up to 99 % of the annual O&M expenses. Pumping energy costs depend on the required distance to transport the concentrate, detailed changes in pumping energy and cost requirements for different concentrate transport distances are included in the supporting information (Fig. S4).

3.3. Deep well injection

The LCCD for representative well depths as a function of concentrate pumping distance are shown in Fig. 9. The LCCD for DWI increases linearly with well depth and transport distance. Because well capacity is defined by well diameter, geohydrological conditions that allow for shallower wells are desirable as drilling, casing, and grouting costs increase with well depth. The lowest LCCD for DWI is 1 $/$m^3$ when pumping is not required for injection and transport is gravity-fed. However, achieving transport by gravity is an improbable scenario because of the minimum injection velocity. The best-case scenario where the LCCD is the lowest at 1.09 $/$m^3$ is when the pumping distance and well depth are minimized. Increasing pumping distance to the upper limit of 35 km results in higher pumping equipment costs and required energy for operation, thus increasing the LCCD by 156 % to 2.64 $/$m^3$. Increasing the well diameter has little impact on the overall LCCD. For example, increasing the well diameter from 16 to 26 cm would almost triple disposal capacity from 3785 to 10,600 m^3/day (1.02 to 2.82 MGD) in the best-case scenario, while only increasing the LCCD by 8 % from 1.09 to 1.19 $/$m^3$. However, in the event of an increase in plant capacity, increasing the well diameter would enable an increased volume of concentrate disposal, which would lower costs because of economy of scale.

The fractional contribution to capital cost for each DWI subsystem component is presented in Fig. 10. The largest contribution to capital cost is for excavation, which includes drilling, casing, and grouting. Casing has the highest cost, ranging from 12 % (0.75 km) to 17 % (3 km) of the capital cost depending on well depth, is required by law for Class I injection wells. The fractional contribution for all other DWI subcomponents costs ranges from 7 % to 14 %. The contribution to cost for components other than excavation has little variation (≈5–6 %) on the capital investment. General O&M costs are calculated as a fixed

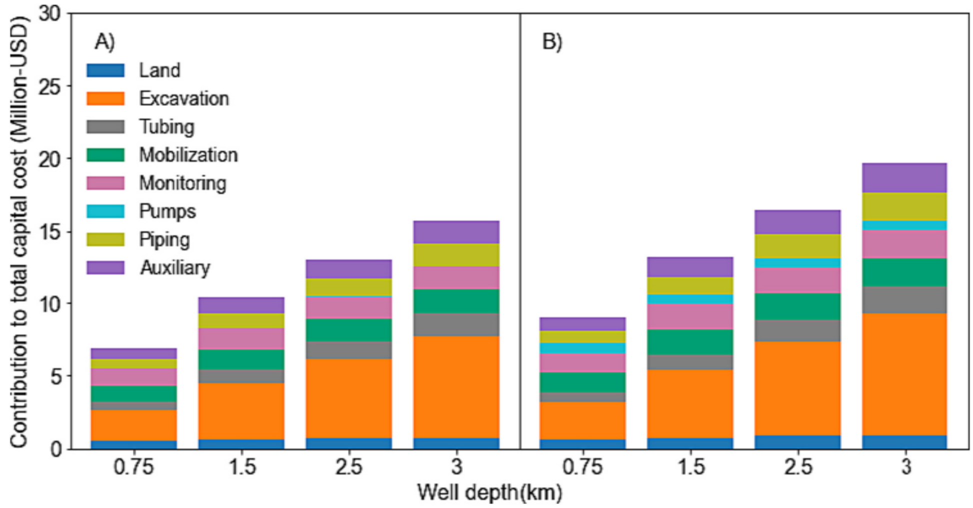

Fig. 10. Contribution to capital cost for DWI subsystem components as a function of well depth for concentrate transport distance a) 1.69 km and b) 35 km. Land costs include purchasing, preparation, and testing. Excavation costs include drilling, casing, and grouting. Excavation costs increase with increasing depth and contribute the most to the capital cost. Although pumping costs increase with transport distance, pumping equipment contribution to capital investment is minimal compared to excavation costs.

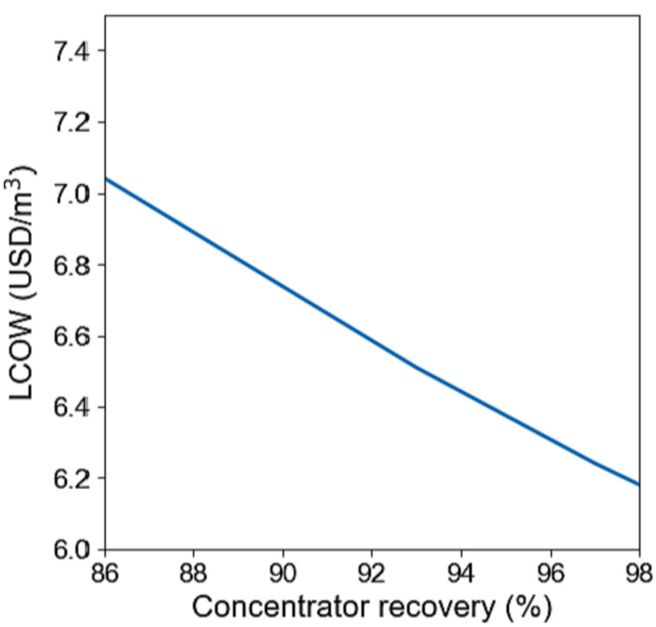

Fig. 11. LCOW as a function of the concentrator working recovery. The concentrator capacity is 3785 m^3/day (1 MGD). Concentrator equipment cost remains constant for the increase in feed salinities. The LCOW decreases with an increase in recovery because of high equipment costs.

percentage of the capital costs and have minimal impact on the LCCD. Detailed costs for pump operation according to concentrate transport distance variations are included in the supporting information (Fig. S4).

3.4. Concentrator

The LCOW for the concentrator system as a function of concentrator recovery is shown in Fig. 11. LCOW decreases with increased recovery because equipment costs are based on system capacity and remain constant for the given feed salinities. From an economic perspective, the best-case scenario is a concentrator working at full recovery (98 %), which results in a LCOW of 6.2 $/$m^{3,}$

The contribution to capital cost and annual O&M by system component is shown in Fig. 12. The main cost driver for capital costs in all cases is the concentrator expenses, which include equipment and installation. The high capital costs result from the need for high-quality anti-corrosion materials and specialized installation needs of the concentrator equipment.

Depending on recovery, the mechanical evaporator equipment and installation costs represent 41 % of the capital investment each. The O&M cost breakdown for the concentrator system is similar to the AGMD system, where thermal energy requirements are the major contribution to O&M with 79 % of annual expenses. The concentrator system O&M costs represent 49 % of the LCOW for all modeled concentrator recoveries. Although the concentrator system takes a waste-to-resource approach, the high cost of equipment, special labor requirements, and high energy requirements make concentrators the least competitive option from an economic perspective.

3.5. System comparison

The LCOW, LCCD, and potential return on investment (ROI) for the best-case scenario for each system are shown in Fig. 13. Results are presented in ascending order of best-case scenarios. For systems with a waste to resource approach (AGMD and concentrator), the LCOW is compared and presented as a positive value contributing to resource maximization. For the conventional concentrate management systems that are based on resource disposal (DWI and evaporation ponds) the LCCD is presented as a negative value to reflect the financial implications of the resource disposal approach.

AGMD with LGH has the lowest LCOW at 0.9 $/$m^3$, followed by AGMD with steam at 1.93 $/$m^3$. Although concentrators have the benefit of recovering water, the LCOW is high at 6.2 $/$m^3$. The lowest LCCD is 1.09 $/$m^3$ for DWI with a minimal depth of 0.75 km, followed by evaporation ponds with lowest transport distance and salinity and highest evaporation rate at 1.42 $/$m^3$. The LCCD are within range of previous studies which have estimated evaporation pond and DWI disposal costs below 10 $/$m^3$ and 2.5 $/$m^3$, respectively [2,10,100]. However, for MD a broad spectrum of costs have been reported anywhere from 0.25 $/$m^3$ to 1.69 $/$m^3$ when waste heat is available and up to 25 $/$m^3$ when an external energy source is needed [2,64,81,101–103]. Similarly, brine concentrator cost estimates range from 0.67 $/$m^3$ to 26.41 $/$m^3$ with and without crystallizers [2,100,104]. The wide range of reported costs is largely because of the different system operating conditions such as system configuration,

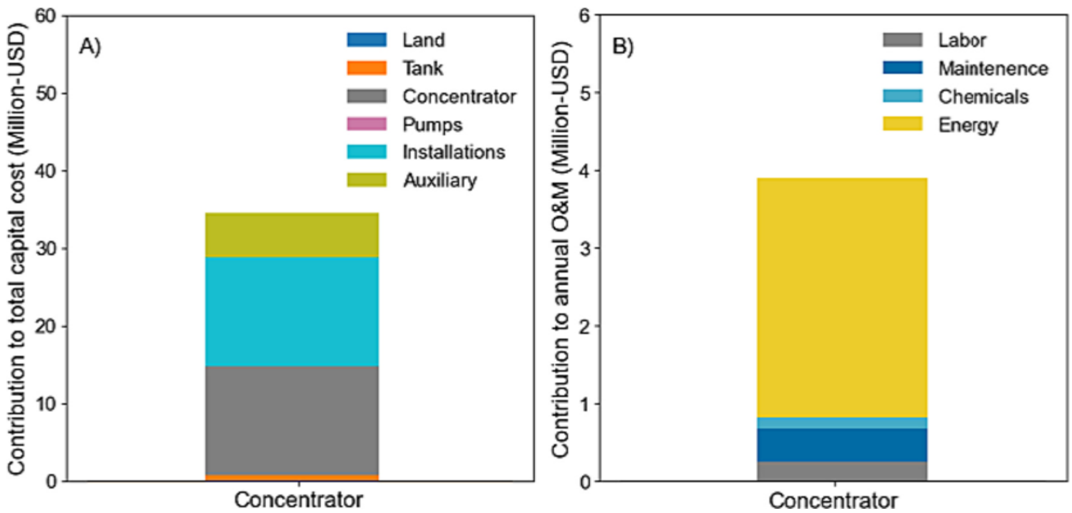

Fig. 12. Fractional contribution system components for a 3785 m^3/day capacity concentrator according to A) capital cost and B) O&M. Operating recovery has little influence on the fractional contribution of the system's components but rather on fixed annual costs as they are dependent on volume of concentrate treated and energy requirements. Equipment and installation costs are the major contributors to capital costs, while thermal energy requirements comprise most of the O&M.

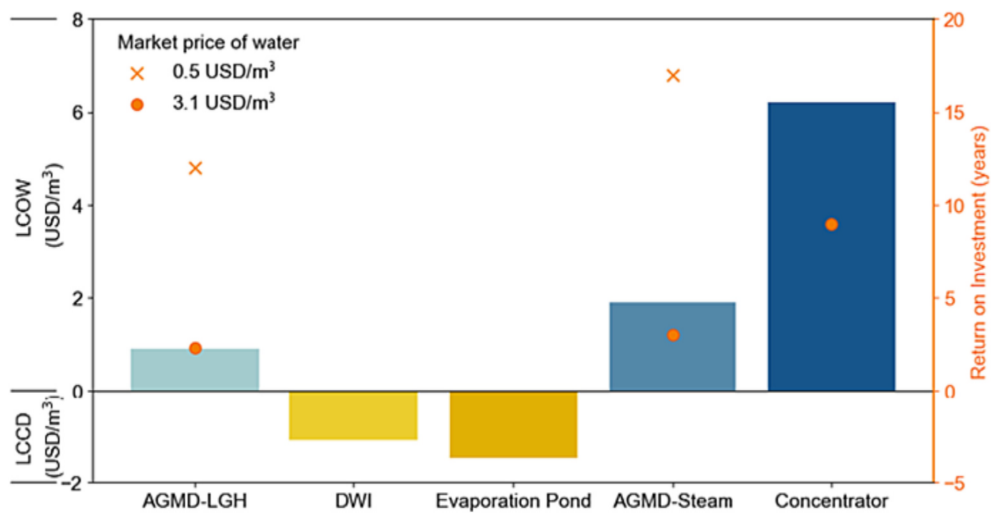

Fig. 13. Fixed cost of concentrate treatment or disposal according to concentrate management system in ascending order. Results are separated as LCOW for systems that place a value on a waste to resource approach such as AGMD and concentrators to aid resource maximization and, and LCCD for systems that take a disposal approach. LCOW are considered positive values to reflect the potential of resource maximization while LCCD are considered negative to reflect the financial implications of the disposal approach. At 0.90 $/$m^3$ AGMD with LGH has the lowest LCOW.

Table 4
Qualitatively comparison of AGMD to established concentrate management technologies for large scale across variable performance metrics. Icon grading scale from 1 to 4 refers to high consumption or cost.

System	Capital cost	Resource recovery	Energy consumption	Modularity	Negative environmental effect
Membrane distillation	●●○○	●●●●	●●●○	●●●●	●○○○
Evaporation pond	●●○○	○○○○	●●○○	○○○○	●●○○
Deep injection well	●●○○	○○○○	●●○○	○○○○	●●○○
Concentrator	●●●●	●●●●	●●●●	●●●○	●●○○

plant capacity, operating temperatures, and concentrate characteristics.

Considering the potential profit for freshwater production from the AGMD and concentrator systems, the ROI can be estimated by considering the market cost of water ranging between 0.5 and 3.1 $/$m^3$ [92]. The ROI for AGMD with LGH and steam would occur at the 12th and 17th years, respectively, for a low market cost of water ($0.5/$m^3$); whereas the ROI for AGMD with LGH and steam would occur at approximately the 2nd and 3rd year, respectively, for a high market cost of water (3.1 $/$m^3$). However, an ROI for the concentrator system would only for the higher water market cost at the 9th year because of the modeled system 20-year lifespan.

Selecting concentrate management technologies solely based on economic metrics neglects consideration of additional performance indicators such as value placed on resource recovery (waste-to-resource approach), energy demands, modularity, global applicability, and potential for adverse environmental impacts. A qualitative comparison of AGMD with the established concentrate management technologies is presented in Table 4. Considering qualitative and quantitative assessments, AGMD with LGH stands as a competitive alternative to conventional concentrate management. Moreover, its waste-to-resource approach not only offsets adverse environmental effects of water treatment facilities on receiving environments but promotes water resource management.

4. Conclusion

A techno-economic assessment was performed to compare AGMD to conventional alternatives for concentrate management. The study results support the economic viability and competitiveness of novel technologies such as AGMD in contrast to current industry practice. Results demonstrate that AGMD is competitive to conventional systems such as evaporation ponds and DWI when longer, more energy efficient modules and LGH are used, resulting in a LCOW of 0.9 $/m^3. In contrast, the LCCD for evaporation ponds and DWI is 1.09 $/m3 and 1.47 $/m^3, respectively, and do not place value on resource recovery. Moreover, AGMD's profit potential via water production further reduces the LCOW and increases AGMD competitiveness to conventional concentrate management technologies.

While AGMD with LGH is a technical and economic alternative for concentrate management, operational considerations such as circulating flow rate and feed salinity, have a large influence on heat and mass transfer in the system which impacts energy requirements, efficiency, water production, and consequently LCOW. Furthermore, AGMD's LCOW increases with the addition of pretreatment strategies and when an external thermal energy sources are required (up to 217 %). Therefore, future techno-economic assessments focusing on the integration of sustainable and renewable energy sources and various pretreatment technologies that enhance AGMD's performance is crucial.

Overall, the modeling framework developed in this study can be adapted to site-specific situations for use in a wide range of hypersaline waste streams and operating conditions from various industries and applications. (e.g., mining, pharmaceutical, energy & oil, data centers), which would aid in alleviating resource depletion by maximizing resource recovery globally to promote water-energy circularity.

CRediT authorship contribution statement

Varinia Felix: Data curation, Formal analysis, Investigation, Methodology, Validation, Writing – original draft, Writing – review & editing. **Mukta Hardikar:** Data curation, Investigation, Methodology. **Kerri L. Hickenbottom:** Conceptualization, Formal analysis, Funding acquisition, Methodology, Project administration, Resources, Supervision, Visualization, Writing – original draft, Writing – review & editing.

Declaration of competing interest

The authors declare that they have no known competing financial interests or personal relationships that could have appeared to influence the work reported in this paper.

Data availability

Data will be made available on request.

Acknowledgments

This research is made possible with support from the Bureau of Reclamation Desalination and Water Purification Research and Development Program Cooperative Agreement No. R18AC00115. The Hickenbottom Environmental Research lab, the University of Arizona Carsons Scholar Program, and CONAHCYT.

Appendix A. Supplementary data

Supplementary data to this article can be found online at https://doi.org/10.1016/j.desal.2023.117213.

References

[1] A. Mushtaque, Brine disposal from inland desalination plants: current status, problems, and opportunities, in: Environmental Sciences and Environmental Computing, 2004. CA. (vol. Volume II of Environmental Sciences and Environmental Computing).
[2] A. Panagopoulos, K.-J. Haralambous, M. Loizidou, Desalination brine disposal methods and treatment technologies - a review, Sci. Total Environ. 693 (2019), 133545, 2019/11/25/, https://doi.org/10.1016/j.scitotenv.2019.07.351.
[3] A. Mushtaque, Brine disposal from inland desalination plants: current status, problems, and opportunities, in: Environmental Sciences and Environmental Computing, 2004. CA. (vol. Volume II of Environmental Sciences and Environmental Computing).
[4] M. Ahmed, W.H. Shayya, D. Hoey, J. Al-Handaly, Brine disposal from reverse osmosis desalination plants in Oman and the United Arab Emirates, Desalination 133 (2) (2001) 135–147, 2001/03/10/, https://doi.org/10.1016/S0011-9164(01)80004-7.
[5] amp Metcalf, I.a.A.C. Eddy, A. Takashi, B. Franklin, L. Harold, Water Reuse: Issues, Technologies, and Applications, First edition. ed., McGraw-Hill Education, New York, 2007 in en.
[6] B.M. Souza-Chaves, et al., Extending the life of water reuse reverse osmosis membranes using chlorination, J. Membr. Sci. 642 (2022), 119897, 2022/02/15/, https://doi.org/10.1016/j.memsci.2021.119897.
[7] M. Mickley, Survey of U.S. Municipal Desalination Facilities, in: 2020 MSSC Annual Salinity Summit. "One Water…It's Here", 2020 ed.
[8] P. Xu, T. Cath, A. Robertson, M. Reinhard, J. Leckie, J. Drewes, Critical review of desalination concentrate management, treatment and beneficial use, Environ. Eng. Sci. 30 (2013) 502–514, 08/01, https://doi.org/10.1089/ees.2012.0348.
[9] A. Giwa, V. Dufour, F. Al Marzooqi, M. Al Kaabi, S.W. Hasan, Brine management methods: recent innovations and current status, Desalination 407 (2017) 1–23, 2017/04/01/, https://doi.org/10.1016/j.desal.2016.12.008.
[10] J. Morillo, J. Usero, D. Rosado, H. El Bakouri, A. Riaza, F.-J. Bernaola, Comparative study of brine management technologies for desalination plants, Desalination 336 (2014) 32–49, 2014/03/03/, https://doi.org/10.1016/j.desal.2013.12.038.
[11] M. Ahmed, W.H. Shayya, D. Hoey, A. Mahendran, R. Morris, J. Al-Handaly, Use of evaporation ponds for brine disposal in desalination plants, Desalination 130 (2) (2000) 155–168, 2000/11/01/, https://doi.org/10.1016/S0011-9164(00)00083-7.
[12] M. Mickley, Treatment of Concentrate. Desalination and Water Purification Research and Development Program Report No. 155, Bureau of Reclamation, Denver, CO, 2008.
[13] M. Mickley, Updated and extended survey of U.S. Municipal desalination plants, in: Desalination and Water Purification Research and Development Program Report No. 207, 2018. Denver, CO.
[14] N. Shammas, C. Sever, L. Wang, Deep-Well Injection for Waste Management, 2010, pp. 521–582.
[15] S. Adham, A. Hussain, J.M. Matar, R. Dores, A. Janson, Application of membrane distillation for desalting brines from thermal desalination plants, Desalination 314 (2013) 101–108, 2013/04/02/, https://doi.org/10.1016/j.desal.2013.01.003.
[16] J.D. Gil, A. Ruiz-Aguirre, L. Roca, G. Zaragoza, M. Berenguel, Prediction models to analyse the performance of a commercial-scale membrane distillation unit for desalting brines from RO plants, Desalination 445 (2018) 15–28, 2018/11/01/, https://doi.org/10.1016/j.desal.2018.07.022.
[17] M. Mickley, Membrane Concentrate Disposal: Practices and Regulation, U.S. Department of the Interior, Bureau of Reclamation, Technical Service Center, Water Treatment Engineering and Research Group, Denver, CO, 2006 [Online]. Available: https://books.google.com/books?id=vE3fRo9bdtUC.
[18] T. Tong, M. Elimelech, The global rise of zero liquid discharge for wastewater management: drivers, technologies, and future directions, Environ. Sci. Technol. 50 (13) (2016) 6846–6855, 2016/07/05, https://doi.org/10.1021/acs.est.6b01000.
[19] Bureau of Reclamation. Brine-Concentrate Treatment and Disposal Options Report. Southern California Regional Brine-Concentrate Management Study Phase I, 2009.
[20] J. Graham, Z. Adam, S. Winnie, R. Parameshwaran, M. Behrooz, N. Michael, Evaluation and Selection of Available Processes for a Zero-Liquid Discharge System for the Perris, California, Ground Water Basin, ed:, U.S. Department of the Interior, Bureau of Reclamation, 2008.
[21] R.K. McGovern, A.M. Weiner, L. Sun, C.G. Chambers, S.M. Zubair, J.H. Lienhard V, On the cost of electrodialysis for the desalination of high salinity feeds, Appl. Energy 136 (2014) 649–661, 2014/12/31/, https://doi.org/10.1016/j.apenergy.2014.09.050.

[22] Y. Zhang, K. Ghyselbrecht, R. Vanherpe, B. Meesschaert, L. Pinoy, B. Van der Bruggen, RO concentrate minimization by electrodialysis: techno-economic analysis and environmental concerns, J. Environ. Manage. 107 (2012) 28–36, 2012/09/30/, https://doi.org/10.1016/j.jenvman.2012.04.020.

[23] G. Cipolletta, N. Lancioni, Ç. Akyol, A.L. Eusebi, F. Fatone, Brine treatment technologies towards minimum/zero liquid discharge and resource recovery: state of the art and techno-economic assessment, J. Environ. Manage. 300 (2021), 113681, 2021/12/15/, https://doi.org/10.1016/j.jenvman.2021.113681.

[24] A. Deshmukh, et al., Membrane distillation at the water-energy nexus: limits, opportunities, and challenges, Energy Environ. Sci. 11 (5) (2018) 1177–1196, https://doi.org/10.1039/C8EE00291F, 10.1039/C8EE00291F.

[25] L. Francis, O. Ogunbiyi, J. Saththasivam, J. Lawler, Z. Liu, A comprehensive review of forward osmosis and niche applications, Environ. Sci. Water Res. Technol. 6 (8) (2020) 1986–2015, https://doi.org/10.1039/D0EW00181C, 10.1039/D0EW00181C.

[26] R. Valladares Linares, et al., Life cycle cost of a hybrid forward osmosis – low pressure reverse osmosis system for seawater desalination and wastewater recovery, Water Res. 88 (2016) 225–234, 2016/01/01/, https://doi.org/10.1016/j.watres.2015.10.017.

[27] M. Mulder, Basic Principles of Membrane Technology, Kluver Academic Publishers, Dordrecht, The Netherlands, 1991.

[28] C.R. Martinetti, A.E. Childress, T.Y. Cath, High recovery of concentrated RO brines using forward osmosis and membrane distillation, in en, J. Membr. Sci. 331 (1) (2009) 31–39, 2009/04/01/, https://doi.org/10.1016/j.memsci.2009.01.003.

[29] G. Naidu, S. Jeong, Y. Choi, S. Vigneswaran, Membrane distillation for wastewater reverse osmosis concentrate treatment with water reuse potential, in en, J. Membr. Sci. 524 (2017) 565–575, 2017/02/15/, https://doi.org/10.1016/j.memsci.2016.11.068.

[30] K.L. Hickenbottom, T.Y. Cath, Sustainable operation of membrane distillation for enhancement of mineral recovery from hypersaline solutions, J. Membr. Sci. 454 (0) (2014) 426–435, 3/15/, https://doi.org/10.1016/j.memsci.2013.12.043.

[31] D.M. Warsinger, J. Swaminathan, E. Guillen-Burrieza, H.A. Arafat, J.H. Lienhard V, Scaling and fouling in membrane distillation for desalination applications: a review, Desalination 356 (2015) 294–313, 2015/01/15/, https://doi.org/10.1016/j.desal.2014.06.031.

[32] L.D. Tijing, Y.C. Woo, J.-S. Choi, S. Lee, S.-H. Kim, H.K. Shon, Fouling and its control in membrane distillation—a review, J. Membr. Sci. 475 (2015) 215–244, 2015/02/01/, https://doi.org/10.1016/j.memsci.2014.09.042.

[33] T. Horseman, Y. Yin, K.S.S. Christie, Z. Wang, T. Tong, S. Lin, Wetting, Scaling, and Fouling in Membrane Distillation: State-of-the-Art Insights on Fundamental Mechanisms and Mitigation Strategies, in: ACS ES&T Engineering, 2020 ed.

[34] M. Hardikar, et al., Membrane distillation provides a dual barrier for coronavirus and bacteriophage removal, Environ. Sci. Technol. Lett. 8 (8) (2021) 713–718.

[35] L. Eykens, T. Reyns, K. De Sitter, C. Dotremont, L. Pinoy, B. Van der Bruggen, How to select a membrane distillation configuration? Process conditions and membrane influence unraveled, Desalination 399 (2016) 105–115, 2016/12/01/, https://doi.org/10.1016/j.desal.2016.08.019.

[36] A.-Z. Mostafa, A comprehensive review of vacuum membrane distillation technique, Desalination 356 (2015) 1–14, 2015/01/15/, https://doi.org/10.1016/j.desal.2014.10.033.

[37] I. Hitsov, K. De Sitter, C. Dotremont, P. Cauwenberg, I. Nopens, Full-scale validated Air Gap Membrane Distillation (AGMD) model without calibration parameters, J. Membr. Sci. 533 (2017) 309–320, 2017/07/01/, https://doi.org/10.1016/j.memsci.2017.04.002.

[38] A.S. Alsaadi, et al., Modeling of air-gap membrane distillation process: a theoretical and experimental study, J. Membr. Sci. 445 (2013) 53–65, 2013/10/15/, https://doi.org/10.1016/j.memsci.2013.05.049.

[39] R.D. Gustafson, J.R. Murphy, A. Achilli, A stepwise model of direct contact membrane distillation for application to large-scale systems: experimental results and model predictions, Desalination 378 (2016) 14–27, 2016/01/15/, https://doi.org/10.1016/j.desal.2015.09.022.

[40] H.C. Duong, P. Cooper, B. Nelemans, T.Y. Cath, L.D. Nghiem, Evaluating energy consumption of air gap membrane distillation for seawater desalination at pilot scale level, Sep. Purif. Technol. 166 (2016) 55–62, 2016/06/22/, https://doi.org/10.1016/j.seppur.2016.04.014.

[41] N. Dow, et al., Pilot trial of membrane distillation driven by low grade waste heat: membrane fouling and energy assessment, Desalination 391 (2016) 30–42, 2016/08/01/, https://doi.org/10.1016/j.desal.2016.01.023.

[42] E. Guillén-Burrieza, G. Zaragoza, S. Miralles-Cuevas, J. Blanco, Experimental evaluation of two pilot-scale membrane distillation modules used for solar desalination, J. Membr. Sci. 409–410 (2012) 264–275, 2012/08/01/, https://doi.org/10.1016/j.memsci.2012.03.063.

[43] J.A. Andrés-Mañas, A. Ruiz-Aguirre, F.G. Acién, G. Zaragoza, Performance increase of membrane distillation pilot scale modules operating in vacuum-enhanced air-gap configuration, Desalination 475 (2020), 114202, 2020/02/01/, https://doi.org/10.1016/j.desal.2019.114202.

[44] A.M. Alklaibi, N. Lior, Comparative study of direct-contact and air-gap membrane distillation processes, Ind. Eng. Chem. Res. 46 (2) (2007) 584–590, 2007/01/01, https://doi.org/10.1021/ie051094u.

[45] M. Hardikar, I. Marquez, T. Phakdon, A.E. Sáez, A. Achilli, Scale-up of membrane distillation systems using bench-scale data, Desalination 530 (2022), 115654, 2022/05/15/, https://doi.org/10.1016/j.desal.2022.115654.

[46] S. Lin, N.Y. Yip, M. Elimelech, Direct contact membrane distillation with heat recovery: thermodynamic insights from module scale modeling, J. Membr. Sci. 453 (2014) 498–515, 2014/03/01/, https://doi.org/10.1016/j.memsci.2013.11.016.

[47] E.K. Summers, H.A. Arafat, J.H. Lienhard, Energy efficiency comparison of single-stage membrane distillation (MD) desalination cycles in different configurations, Desalination 290 (2012) 54–66, 2012/03/30/, https://doi.org/10.1016/j.desal.2012.01.004.

[48] A. Alkhudhiri, N. Darwish, N. Hilal, Membrane distillation: a comprehensive review, Desalination 287 (2012) 2–18, 2012/02/15/, https://doi.org/10.1016/j.desal.2011.08.027.

[49] V. Karanikola, S.E. Moore, A. Deshmukh, R.G. Arnold, M. Elimelech, A.E. Sáez, Economic performance of membrane distillation configurations in optimal solar thermal desalination systems, Desalination 472 (2019), 114164, 2019/12/15/, https://doi.org/10.1016/j.desal.2019.114164.

[50] R.D. Gustafson, S.R. Hiibel, A.E. Childress, Membrane distillation driven by intermittent and variable-temperature waste heat: system arrangements for water production and heat storage, Desalination 448 (2018) 49–59, 2018/12/15/, https://doi.org/10.1016/j.desal.2018.09.017.

[51] X. Cheng, et al., Effects of pre-ozonation on the ultrafiltration of different natural organic matter (NOM) fractions: membrane fouling mitigation, prediction and mechanism, J. Membr. Sci. 505 (2016) 15–25.

[52] H. Zhu, X. Wen, X. Huang, Membrane organic fouling and the effect of pre-ozonation in microfiltration of secondary effluent organic matter, J. Membr. Sci. 352 (1–2) (2010) 213–221.

[53] M. Park, T. Anumol, J. Simon, F. Zraick, S.A. Snyder, Pre-ozonation for high recovery of nanofiltration (NF) membrane system: membrane fouling reduction and trace organic compound attenuation, J. Membr. Sci. 523 (2017) 255–263, 2017/02/01/, https://doi.org/10.1016/j.memsci.2016.09.051.

[54] M.R. Choudhury, N. Anwar, D. Jassby, M.S. Rahaman, Fouling and wetting in the membrane distillation driven wastewater reclamation process – a review, Adv. Colloid Interface Sci. 269 (2019) 370–399, 2019/07/01/, https://doi.org/10.1016/j.cis.2019.04.008.

[55] K. Rajwade, A.C. Barrios, S. Garcia-Segura, F. Perreault, Pore wetting in membrane distillation treatment of municipal wastewater desalination brine and its mitigation by foam fractionation, in en, Chemosphere 257 (2020), 127214, 2020/10/01/, https://doi.org/10.1016/j.chemosphere.2020.127214.

[56] M.E.A. Ali, R. Alghanayem, A. Varela, M. Bellier, F. Perreault, Scaling mitigation in direct contact membrane distillation using air microbubbles, Desalination 549 (2023), 116348, 2023/03/01/, https://doi.org/10.1016/j.desal.2022.116348.

[57] L. Presson, V. Felix, M. Hardikar, A. Achilli, K.L. Hickenbottom, Fouling Characterization and Treatment of Water Reuse Concentrate with Membrane Distillation: Do Organics Really Matter, Available at SSRN 4279583, 2022.

[58] M. Hardikar, I. Marquez, A. Achilli, Emerging investigator series: membrane distillation and high salinity: analysis and implications, Environ. Sci. Water Res. Technol. 6 (6) (2020) 1538–1552, https://doi.org/10.1039/C9EW01055F, 10.1039/C9EW01055F.

[59] G. Naidu, X. Zhong, S. Vigneswaran, Comparison of membrane distillation and freeze crystallizer as alternatives for reverse osmosis concentrate treatment, Desalination 427 (2018) 10–18, 2018/02/01/, https://doi.org/10.1016/j.desal.2017.10.043.

[60] A. Abdel-Karim, S. Leaper, C. Skuse, G. Zaragoza, M. Gryta, P. Gorgojo, Membrane cleaning and pretreatments in membrane distillation – a review, Chem. Eng. J. 422 (2021), 129696, 2021/10/15/, https://doi.org/10.1016/j.cej.2021.129696.

[61] R.B. Saffarini, E.K. Summers, H.A. Arafat, J.H. Lienhard V, Economic evaluation of stand-alone solar powered membrane distillation systems, Desalination 299 (2012) 55–62, 2012/08/01/, https://doi.org/10.1016/j.desal.2012.05.017.

[62] K.L. Hickenbottom, et al., Techno-economic assessment of a closed-loop osmotic heat engine, J. Membr. Sci. 535 (2017) 178–187, 2017/08/01/, https://doi.org/10.1016/j.memsci.2017.04.034.

[63] S.E. Moore, S.D. Mirchandani, V. Karanikola, T.M. Nenoff, R.G. Arnold, A. Eduardo Sáez, Process modeling for economic optimization of a solar driven sweeping gas membrane distillation desalination system, Desalination 437 (2018) 108–120, 2018/07/01/, https://doi.org/10.1016/j.desal.2018.03.005.

[64] D. Amaya-Vías, J.A. López-Ramírez, Techno-economic assessment of air and water gap membrane distillation for seawater desalination under different heat source scenarios, Water 11 (10) (2019), https://doi.org/10.3390/w11102117.

[65] G. Zaragoza, J.A. Andrés-Mañas, A. Ruiz-Aguirre, Commercial scale membrane distillation for solar desalination, npj Clean Water 1 (1) (2018) 20, 2018/10/30, https://doi.org/10.1038/s41545-018-0020-z.

[66] M. Hardikar, et al., Pore flow and solute rejection in pilot-scale air-gap membrane distillation, J. Membr. Sci. 676 (2023), 121544.

[67] M. Hardikar, V. Felix, A.B. Rabe, L.A. Ikner, K.L. Hickenbottom, A. Achilli, Virus rejection and removal in pilot-scale air-gap membrane distillation, Water Res. 240 (2023), 120019, 2023/07/15/, https://doi.org/10.1016/j.watres.2023.120019.

[68] J.A. Andrés-Mañas, I. Requena, G. Zaragoza, Characterization of the use of vacuum enhancement in commercial pilot-scale air gap membrane distillation modules with different designs, Desalination 528 (2022), 115490, 2022/04/15/, https://doi.org/10.1016/j.desal.2021.115490.

[69] E. Guillén-Burrieza, et al., Experimental analysis of an air gap membrane distillation solar desalination pilot system, J. Membr. Sci. 379 (1) (2011) 386–396, 2011/09/01/, https://doi.org/10.1016/j.memsci.2011.06.009.

[70] J.A. Andrés-Mañas, I. Requena, G. Zaragoza, Membrane distillation of high salinity feeds: steady-state modelling and optimization of a pilot-scale module in vacuum-assisted air gap operation, Desalination 553 (2023), 116449, 2023/05/01/, https://doi.org/10.1016/j.desal.2023.116449.

[71] M. Inkawhich, J. Shingler, R.S. Ketchum, W. Pan, R.A. Norwood, K. L. Hickenbottom, Temporal performance indicators for an integrated pilot-scale membrane distillation-concentrated solar power/photovoltaic system, Appl. Energy 349 (2023), 121675, 2023/11/01/, https://doi.org/10.1016/j.apenergy.2023.121675.
[72] U. Kesieme, N.A. Milne, H. Aral, C.Y. Cheng, M.C. Duke, Novel Application of Membrane Distillation for Acid and Water Recovery From Mining Waste Waters, 2012.
[73] I.-E. Noor, A. Martin, O. Dahl, Techno-economic system analysis of membrane distillation process for treatment of chemical mechanical planarization wastewater in nano-electronics industries, Sep. Purif. Technol. 248 (2020), 117013, 2020/10/01/, https://doi.org/10.1016/j.seppur.2020.117013.
[74] S. Tavakkoli, O.R. Lokare, R.D. Vidic, V. Khanna, A techno-economic assessment of membrane distillation for treatment of Marcellus shale produced water, Desalination 416 (2017) 24–34, 2017/08/15/, https://doi.org/10.1016/j.desal.2017.04.014.
[75] S. Kalla, Use of membrane distillation for oily wastewater treatment – a review, J. Environ. Chem. Eng. 9 (1) (2021), 104641, 2021/02/01/, https://doi.org/10.1016/j.jece.2020.104641.
[76] X. Li, Y. Mo, W. Qing, S. Shao, C.Y. Tang, J. Li, Membrane-based technologies for lithium recovery from water lithium resources: a review, J. Membr. Sci. 591 (2019), 117317, 2019/12/01/, https://doi.org/10.1016/j.memsci.2019.117317.
[77] D.W. Green, R.H. Perry, Perry's Chemical Engineers' Handbook, Eighth Edition, McGraw-Hill Education, 2007.
[78] Aquastil, AQ21US01 Manual of Operation, ed., Sittard NL, 2021.
[79] J.A. Andrés-Mañas, I. Requena, A. Ruiz-Aguirre, G. Zaragoza, Performance modelling and optimization of three vacuum-enhanced membrane distillation modules for upscaled solar seawater desalination, Sep. Purif. Technol. 287 (2022), 120396, 2022/04/15/, https://doi.org/10.1016/j.seppur.2021.120396.
[80] A.S. NL, Membrane Distillation Module Costing, ed, 2022.
[81] S. Al-Obaidani, E. Curcio, F. Macedonio, G. Di Profio, H. Al-Hinai, E. Drioli, Potential of membrane distillation in seawater desalination: thermal efficiency, sensitivity study and cost estimation, J. Membr. Sci. 323 (2008) 85–98, 10/01, https://doi.org/10.1016/j.memsci.2008.06.006.
[82] E.C. Wert, S. Gonzales, M.M. Dong, F.L. Rosario-Ortiz, Evaluation of enhanced coagulation pretreatment to improve ozone oxidation efficiency in wastewater, Water Res. 45 (16) (2011) 5191–5199, 2011/10/15/, https://doi.org/10.1016/j.watres.2011.07.021.
[83] A. Shubert, Overview of the El Paso Kay Bailey Hutchison desalination plant, in: Texas Desal Conference, Austin Texas, El Paso Water Utilities, 2015.
[84] N. W. Service, Climate Zones. https://www.weather.gov/jetstream/climates (accessed 2023).
[85] C.G. Keyes, M.P. Fahy, B. Tansel, Concentrate Management in Desalination: Case Studies, American Society of Civil Engineers. Environmental Water Resources Institute. Task Committee on Development of Prestandards for Concentrate Management Case Studies, 2012 [Online]. Available: https://books.google.com/books?id=fAY0zwEACAAJ.
[86] W. Hutchison, El Paso Water Utilities. Deep-Well Injection of Desalination Concentrate in El Paso, Texas.
[87] S.R. Alan, Overview of the El Paso Kay Bailey Hutchison Desalination Plant. Texas Desal Conference, ed, October, 2015.
[88] J. Graham, Z. Adam, S. Winnie, R. Parameshwaran, N. Michael, in: U. S. D. o. t. I. B. o. Reclamation (Ed.), Evaluation and Selection of Available Processes for a Zero-Liquid Discharge System for the Perris, California, Ground Water Basin. Report 149, April, 2008 ed.
[89] V.W. Technologies, HPD® Evaporation & Crystallization. https://www.veoliawatertech.com/EN-US (accessed 2023).
[90] United, States Bureau of Labor Statistics Occupational Employment and Wage Statistics, Division of Occupational Employment and Wage Statistics, March, 2021 [Online]. Available: https://www.bls.gov/oes/current/oes518091.htm.
[91] A. Goodrich, T. James, M. Woodhouse, Residential, Commercial, and Utility-Scale Photovoltaic (PV) System Prices in the United States: Current Drivers and Cost-Reduction Opportunities, 2012.
[92] A. Panagopoulos, Techno-economic assessment of zero liquid discharge (ZLD) systems for sustainable treatment, minimization and valorization of seawater brine, J. Environ. Manage. 306 (2022), 114488, 2022/03/15/, https://doi.org/10.1016/j.jenvman.2022.114488.
[93] D.E. Garrett, Chemical Engineering Economics/Donald E. Garrett, no. Accessed from, https://nla.gov.au/nla.cat-vn1959065, Van Nostrand Reinhold, New York, .
[94] M.S. Peters, K.D. Timmerhaus, Plant Design and Economics for Chemical Engineers, McGraw-Hill Education, 2003.
[95] M.S. Peters, K.D. Timmerhaus, Plant Design and Economics for Chemical Engineers, McGraw-Hill Education, 2003.
[96] G. Towler, R. Sinnott, Chemical Engineering Design: Principles, Practice and Economics of Plant and Process Design, Butterworth-Heinemann, 2021.
[97] C. Branan, Rules of Thumb for Chemical Engineers: A Manual of Quick, Accurate Solutions to Everyday Process Engineering Problems, Gulf Professional Pub, 2002.
[98] C. Haslego, G. Polley, Compact heat exchangers-part 1: designing plate-and-frame heat exchangers, Chem. Eng. Prog. 98 (9) (2002) 32–37.
[99] S. Sethi, M. Wiesner, Cost modeling and estimation of crossflow membrane filtration processes, Environ. Eng. Sci. 17 (2000) 61–79, 03/01, https://doi.org/10.1089/ees.2000.17.61.
[100] L.F. Greenlee, D.F. Lawler, B.D. Freeman, B. Marrot, P. Moulin, Reverse osmosis desalination: water sources, technology, and today's challenges, Water Res. 43 (9) (2009) 2317–2348, 2009/05/01/, https://doi.org/10.1016/j.watres.2009.03.010.
[101] G.W. Meindersma, C.M. Guijt, A.B. de Haan, Desalination and water recycling by air gap membrane distillation, Desalination 187 (1) (2006) 291–301, 2006/02/05/, https://doi.org/10.1016/j.desal.2005.04.088.
[102] G. Zuo, G. Guan, R. Wang, Numerical modeling and optimization of vacuum membrane distillation module for low-cost water production, Desalination 339 (2014) 1–9, 2014/04/15/, https://doi.org/10.1016/j.desal.2014.02.005.
[103] R. Schwantes, K. Chavan, D. Winter, C. Felsmann, J. Pfafferott, Techno-economic comparison of membrane distillation and MVC in a zero liquid discharge application, Desalination 428 (2018) 50–68, 2018/02/15/, https://doi.org/10.1016/j.desal.2017.11.026.
[104] J. Rioyo, V. Aravinthan, J. Bundschuh, M. Lynch, A review of strategies for RO brine minimization in inland desalination plants, Desalin. Water Treat. 90 (2017) 110–123.